

See discussions, stats, and author profiles for this publication at: <https://www.researchgate.net/publication/43048248>

# X-ray Diffraction Imaging of Anatase and Rutile

ARTICLE *in* ANALYTICAL CHEMISTRY · APRIL 2010

Impact Factor: 5.64 · DOI: 10.1021/ac9024126 · Source: PubMed

---

CITATIONS

14

READS

137

## 2 AUTHORS:



Kenji Sakurai

National Institute for Materials Science

158 PUBLICATIONS 982 CITATIONS

[SEE PROFILE](#)



Mari Mizusawa

CROSS-Tokai

31 PUBLICATIONS 51 CITATIONS

[SEE PROFILE](#)

# X-ray Diffraction Imaging of Anatase and Rutile

Kenji Sakurai\* and Mari Mizusawa

National Institute for Materials Science (NIMS), 1-2-1 Sengen, Tsukuba, Ibaraki 305-0047, Japan

Both anatase and rutile are well-known as stable phases of  $\text{TiO}_2$ . In real-life samples,  $\text{TiO}_2$  is most likely to be a mixture of those phases rather than pure anatase and rutile, and therefore quantitative analysis is extremely important. It is basically possible to determine the average ratio by X-ray diffraction (XRD) using differences in the crystal structure, but it is not easy to do so when attempting mapping by point-by-point scanning. The present paper describes the successful application of newly developed projection-type XRD imaging, which is an extremely rapid and highly efficient method.

The powder X-ray diffraction (XRD) technique is one of the most powerful scientific tools for identifying and quantifying various kinds of crystalline materials.<sup>1–3</sup> The method has been also used for analyzing the concentration and/or the absolute amount of a mixture, where each component has the same or a fairly similar chemical composition but the crystal structure differs. Since the early days of modern materials chemistry, even in the 1950s, quantitative analysis of a mixture of anatase and rutile, both of which are well-known stable phases of titanium dioxide ( $\text{TiO}_2$ ), has been done by XRD.<sup>4,5</sup> In real-life applications,  $\text{TiO}_2$  is most likely to be a mixture rather than pure anatase and rutile.<sup>6</sup> Furthermore, the control of the transformation between anatase and rutile is one of the most important issues in synthesis.<sup>7</sup> Typically, ordinary XRD techniques need uniform samples for measurement and analysis. In the case of a mixture of several materials, it is usually assumed that the concentration (or the weight) ratio is almost the same for all points in the mixture sample. However, as is often the case for thin films and powders, real samples are not always uniform. One needs information in the form of a map rather than a single value of the ratio for such cases. To make a map of the fraction ratio of anatase (or rutile), it is necessary to make repeated XRD measurements with a small X-ray beam for all points in the interested area. Recent advances in micro and nanobeam

optics<sup>8,9</sup> have brought great opportunities for extending many X-ray techniques to 2D analysis. Such analysis can give full information on complicated inhomogeneous mixed systems. However, unfortunately, the technique still requires XY scans, resulting in limitations because of the fairly long measurement required, especially when the number of points increases. In the present article, we describe a novel quick way of mapping nonuniform anatase–rutile mixtures. The technique employed is so-called projection-type XRD imaging, which is an extremely rapid and efficient technique, developed through a series of pioneering works by Wroblewski.<sup>10–15</sup> The method does not require any XY scan of the sample or X-ray beam. Instead, it uses a camera system whereby each pixel always corresponds to a specific position on the sample. We demonstrate the feasibility of quantitative mapping of anatase and rutile.

## EXPERIMENTAL SECTION

A pellet was prepared by a press (5000 kg, 10 min) in order to create two different samples of an anatase–rutile mixture. Samples 1 and 2 were located at specific positions, as shown in the inset of Figure 1. In order to make a good pellet, 100 mg of cellulose was used as a binder for 198 mg of the sample powders. Samples 1 and 2 are anatase-rich and rutile-rich mixtures, respectively, though actually they were commercially available powders of anatase (99.9% purity, average particle size  $\sim 5 \mu\text{m}$ , Wako Chemical) and rutile (99.9% purity, particle size 5–30  $\mu\text{m}$ , Wako Chemical), respectively. However, as will be shown later, their purity was unsatisfactory, and both of them were a mixture of anatase and rutile.

In the present study, a synchrotron X-ray beam was used. The experiments were performed with a flat Si (111) double-crystal monochromator at the multipole-wiggler beamline, BL-16A1, Photon Factory, KEK, Japan. The beamline provides extremely high intensity X-ray photons in 7–15 keV range. Though the present experiments were done with rather low energy (around 5 keV), it was still possible to obtain clear X-ray images. The projection-type X-ray imaging system employed was essentially the same as

- \* To whom correspondence should be addressed. E-mail: sakurai@yuhgiri.nims.go.jp.
- (1) Guinebretiere, R. *X-Ray Diffraction by Polycrystalline Materials*; ISTE Publishing: London, 2007.
  - (2) Jenkins, R.; Snyder, R. L. *Introduction to X-Ray Powder Diffractometry*; John Wiley & Sons: London, 1996.
  - (3) Cullity, B. D. *Elements of X-ray Diffraction*; Addison-Wesley: Reading, MA, 1956.
  - (4) Spurr, F. A.; Myers, H. *Anal. Chem.* **1957**, 29, 760.
  - (5) Chung, F. H. J. *Appl. Crystallogr.* **1974**, 7, 519.
  - (6) Bakardjieva, S.; Subrt, J.; Stengl, V.; Dianez, M. J.; Sayagues, M. J. *Appl. Catal., B* **2005**, 58, 193.
  - (7) Czanderna, A. W.; Rao, C. N. R.; Honig, J. M. *Trans. Faraday Soc.* **1958**, 7, 1069.

- (8) MacDowell, A. A.; Celestre, R. S.; Tamura, N.; Spolenak, R.; Valek, B.; Brown, W. L.; Bravman, J. C.; Padmore, H. A.; Batterman, B. W.; Patel, J. R. *Nucl. Instrum. Methods* **2001**, A467–468, 936.
- (9) *In Nat. Mater.*, **2009**, 8 (4), the Insight section features a compilation of articles on recent electron and X-ray microscopy.
- (10) Wroblewski, T.; Geier, S.; Hessmer, R.; Schreck, M.; Rauschenbach, B. *Rev. Sci. Instrum.* **1995**, 66, 3560.
- (11) Wroblewski, T. *Synchrotron Rad. News* **1996**, 9, 14.
- (12) Wroblewski, T.; Breuer, D.; Crostack, H. A.; Fandrich, F.; Gross, M.; Klimanek, P. *Mater. Sci. Forum* **1998**, 278–281, 216.
- (13) Wroblewski, T.; Woldt, E. *Adv. X-Ray Anal.* **1999**, 40 CD-ROM.
- (14) Wroblewski, T.; Woldt, E. *Adv. X-Ray Anal.* **2001**, 42, 258.
- (15) Wroblewski, T. *Mater. Sci. Forum* **2002**, 404–407, 121.

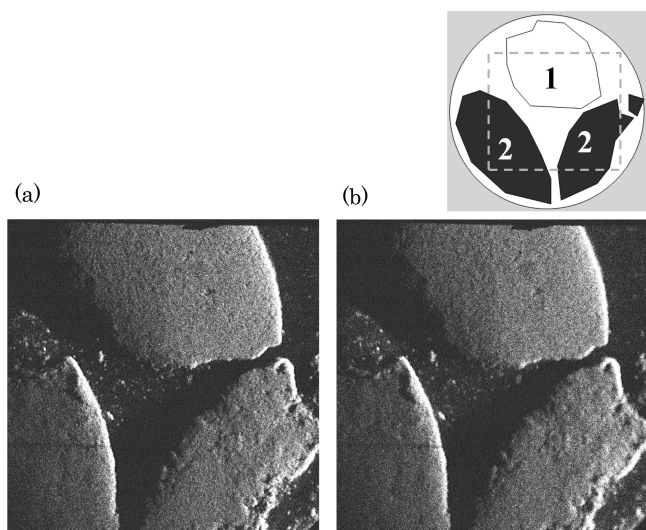


**Figure 1.** X-ray images measured with 5400 eV X-rays at diffraction angles of (a) 84 deg and (b) 76 deg, respectively. The area size is 8 mm × 8 mm. Exposure time and repetition are 1 s and 30 times, respectively. The background (due to electronic noise) is subtracted after summing 30 images. The inset shows the schematic of the location of samples 1 and 2 in the pellet.

those used for X-ray fluorescence<sup>16,17</sup> and X-ray absorption fine structure (XAFS),<sup>18,19</sup> which were developed at the National Institute for Materials Science (NIMS), Tsukuba Japan. In short, the instrument combines small-angle-incidence geometry (0–2 deg) using a rather wide beam (0.6 mm (vertical) × 8 mm (horizontal)) and parallel optics (~6 mrad) for detecting X-rays by a fast CCD camera (Texas Instruments TC281, exposure area 1024 × 1024 pixels, pixel size 8 μm squared, Peltier cooling –30 °C). Further instrumental details were described elsewhere.<sup>16–18</sup> In most previous studies, the camera was fixed at almost a 90 deg position extremely close to the sample surface,<sup>20</sup> but this time, the goniometer was used to change the angle from a 90 deg position. Two angles were chosen, 84 and 76 deg, to observe the anatase 200 and rutile 210 reflections, respectively, for 4900 eV X-rays. Measurement was quick, and the time for reading out even reached a speed of 30 frames/s. Here, the spatial resolution is determined by the accepting angular divergence of diffracted X-rays for each pixel and the sample–detector distance, rather than the pixel size of the detector. This is typically around 15 μm but was somewhat worse in the present study because of the slightly longer sample–detector distance due to the deviation from the 90 deg position. An X-ray powder diffractometer (Rigaku RINT Ultima III, Cu tube with Ni filter, without monochromator, 40 kV–30 mA) was also employed to measure the diffraction patterns of samples 1 and 2.

## RESULTS AND DISCUSSION

Parts a and b of Figure 1 show X-ray images of the anatase–rutile pellet samples, measured with 5400 eV X-rays at diffraction angles of 84 deg and 76 deg, respectively. The images were taken without moving anything, samples, camera, or any of

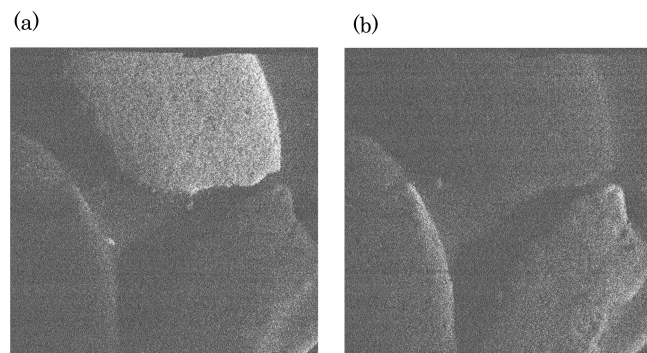


**Figure 2.** X-ray images measured with 4900 eV X-rays at diffraction angles of (a) 84 deg and (b) 76 deg, respectively, which correspond to anatase 200 and rutile 210 images. The area size is 8 mm × 8 mm. Exposure time and repetition are 1 s and 100 times, respectively.

the other optics. In this case, the incident X-ray energy is higher than that of the Ti-K absorption edge (4965 eV), and therefore the images are mainly due to X-ray fluorescence from titanium. As clearly seen in both images, the regions for both samples 1 and 2 are bright. They are a map of the Ti concentration but do not distinguish between parts a and b of Figure 1, as the difference in projection angle was only 8 deg. On the other hand, the right-hand edges appear bright in the images. This is because the X-rays came from the right-hand side and produce scattering at the edges. Basically, it is possible to correct for such effects on the images by taking several exposures with different rotation angles in the plane.

Parts a and b of Figure 2 show X-ray images of the same samples, measured with 4900 eV X-rays at diffraction angles of 84 deg and 76 deg, respectively. As mentioned earlier, these two angles give diffraction peaks for  $d$  values of 1.89 (anatase 200) and 2.05 Å (rutile 210), respectively. At 84 deg, the sample 1 region becomes bright because the major component of sample 1 is anatase. In the same way, at 76 deg, the sample 2 region is bright. Because of rather weak intensity of the primary X-rays at this energy, observed X-ray intensity level was not much higher than the dark current level. We needed 100 times of repetition for the exposure, which is not usual for this imaging system. As X-ray fluorescence from titanium is suppressed completely, the observed X-rays are mostly X-ray diffraction. The analytical depth is estimated at around 2 μm. It is quite shallow because of small angle incidence, though the absorption is basically small because of the low energy side of the absorption edge. The two images correspond roughly to maps of anatase and rutile, respectively. Fairly good agreement with the optical microscope images was confirmed. In this way, the present technique can give an image showing which area satisfies the X-ray diffraction condition of the specific material. The method does not require any XY scans of the sample, and therefore, one of the biggest advantages is the capability of quick surveying of an anatase (or rutile) high-concentration area in the sample.

In the practical analysis, one would need quantitative information such as the fraction ratio of the anatase,  $f$  (= anatase weight / (anatase weight + rutile weight)). Figure 3 shows powder X-ray diffraction patterns of samples 1 and 2 measured by a laboratory X-ray source. Although both chemicals are sold as pure materials, one can see both anatase and rutile peaks, indicating that they

(16) Sakurai, K. *Spectrochim. Acta B* 1999, 54, 1497.

(17) Sakurai, K.; Eba, H. *Anal. Chem.* 2003, 75, 355.

(18) Sakurai, K.; Mizusawa, M. *Nanotechnology* 2004, S428, 15.

(19) Mizusawa, M.; Sakurai, K. *J. Synchrotron Rad.* 2004, 11, 209.

(20) Sakurai, K.; Mizusawa, M. *AIP Conf. Proc.* 2004, 705, 809.

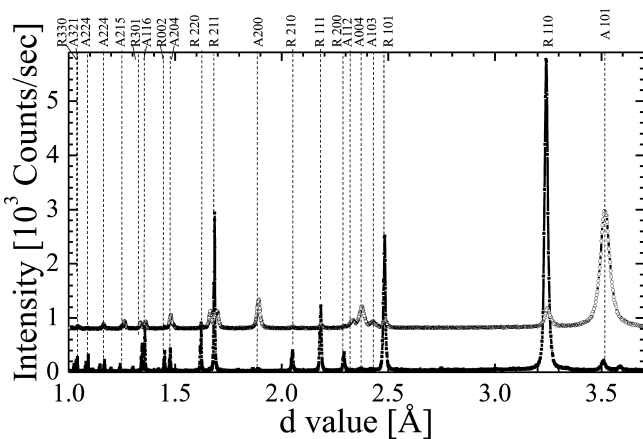


**Figure 3.** Powder X-ray diffraction patterns of samples 1 (○) and 2 (■) measured with CuK $\alpha$  (8.04 keV). The data are displayed as a function of the  $d$  value by  $d = \lambda/(2 \sin \theta)$ .

**Table 1. Measured Intensity of Anatase and Rutile Diffraction Lines for Samples 1 and 2<sup>a</sup>**

	intensity [cps]				$f$
	anatase 101	anatase 200	rutile 110	rutile 210	$f$
sample 1	64 132.3	16 855.7	6 432.5	575.5	0.89
sample 2	1 788.5	393.3	53 883.3	3 199.5	0.03

<sup>a</sup> The intensity is net integrated intensity (after subtracting background)  $f$  is a fraction ratio of the anatase, (anatase weight/(anatase weight + rutile weight)), determined from the intensity ratio of the anatase 101 and rutile 110 reflections.

are a mixture. According to the literature,<sup>4</sup> the intensity ratio between anatase 101,  $I_{A101}$  and rutile 110,  $I_{R110}$ , which are the strongest peaks, gives the following relation,  $f = 1/(1 + 1.26(I_{R110})/(I_{A101}))$ . As summarized in Table 1,  $f$  for samples 1 and 2 is found to be 0.89 and 0.03, respectively. Both values are averages for whole powders. Similar analysis can be introduced into X-ray images shown in Figure 2a,b. Here, let us consider the intensity ratio between anatase 200,  $I_{A200}$  and rutile 210,  $I_{R210}$ , for 4900 eV X-rays, at each point  $(x, y)$ . The formula can be written as

$$f(x, y) = \frac{1}{1 + \alpha \frac{I_{R210}(x, y)}{I_{A200}(x, y)}}$$

From Table 1, we found that the ratios  $I_{A200}/I_{A101}$  and  $I_{R210}/I_{R110}$  are 0.26 and 0.06, respectively, for Cu K $\alpha$  (8404 eV). The

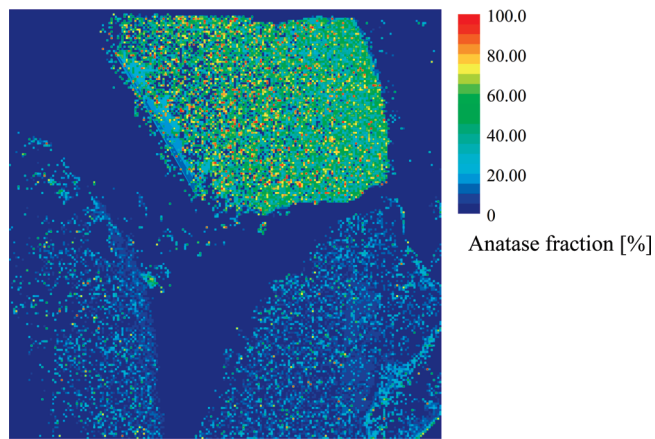


**Figure 4.** Image of the anatase fraction produced from Figure 2a,b.

values are in good agreement with many reports in the JCPDS database. Furthermore the Lorentz-polarization factor should be taken into account because the present experiments used horizontally polarized synchrotron beam and a double crystal monochromator, and X-ray energy (i.e., Bragg angle) is different. The values are summarized in Table 2. The influence of this effect is around 0.567 and 0.519 for  $I_{A200}$  and  $I_{R210}$ , respectively. Then,  $\alpha$  is found to be 5.0.

The procedure for the quantitative mapping is as follows: (i) integration of  $5 \times 5$  pixels for 6 images (84 deg, 76 deg, and dark images for 5400 and 4900 eV), (ii) producing 4 images (similar to Figures 1a,b and 2a,b with reduced pixel numbers) by subtraction of dark images in (i), (iii) calculating  $f(x, y)$  for  $(x, y)$  which shows some level of intensity in 5400 eV images. To obtain a quantitative map, some integration is certainly necessary. Although Figure 2a,b basically give maps of  $I_{A200}$  and  $I_{R210}$ , this does not mean a very strict 1:1 correspondence between the sample position and the X-ray diffraction image because the sample is the randomly oriented powders. Even when some area in the sample is filled with the same material, all pixels in the area will not be always bright. When some powders satisfy the diffraction condition, neighboring powders may not diffract X-rays because of the orientation difference. To avoid such a problem common to the powder samples, some integration will be necessary. In the present study, X-ray intensity was integrated in  $5 \times 5$  pixels. Figure 4 shows the map of the anatase fraction ratio that was finally obtained. The image appears to be similar to Figure 2a but gives quantitative information on the anatase and rutile ratio. It has been found that the average values of  $f$  for the anatase-rich

**Table 2. Correction of Lorentz-Polarization Factor<sup>a</sup>**

	anatase 200		rutile 210	
	Bragg angle (deg)	Lorentz-polarization factor	Bragg angle (deg)	Lorentz-polarization factor
unpolarized CuK $\alpha$	24.042	2.385	22.062	2.897
horizontally polarized (90%) monochromatized 4900 eV (Bragg angle for Si(111) double crystal monochromator 23.8 deg) ratio	42.019	1.352	38.107	1.504
		0.567		0.519

<sup>a</sup> As the experiments were done at synchrotron beamline, differences in Lorentz-polarization factors need to be taken into consideration.

(sample 1) and rutile-rich (sample 2) regions were around 0.5 and 0.07. They do not agree very well with those determined from ordinary powder X-ray diffraction, i.e., 0.89 and 0.03 (in Table 1). One of the reasons for these errors is the rather weak signal intensity compared with the dark current level. In this analysis, we tried to take an X-ray intensity ratio obtained at two different angles, but both intensities are not very high compared with the dark current level. The use of much higher photon flux could solve this problem. When such statistical errors are small enough, the precision of the anatase fraction ratio at each pixel will be a few percentages, similar to the case of ordinary powder X-ray diffraction of the uniformly mixed sample.<sup>4</sup> There might be other factors which can give some influence on the quantitative analysis. In samples 1 and 2, in addition to anatase and rutile, there is quite a large amount of cellulose powder, which could produce some X-ray scattering. Such background can be responsible for the error. X-ray fluorescence from Ti is basically suppressed, but some contribution by higher order harmonics of the primary X-ray beam can increase the background. However, even under nonideal experimental conditions, one can obtain a very clear map for the anatase fraction value shown in Figure 4.

From a methodological point of view, XRD imaging can be done without changing the diffraction angle.<sup>21</sup> In this case, the energy scan of the X-ray beam is employed. If 90 deg is chosen as a diffraction angle, one needs to use the Bragg energy, i.e.,  $E [\text{keV}] = 12.3981/(2d [\text{\AA}] \sin (45[\text{deg}]))$ , where  $d$  is a corresponding lattice parameter. However, in the present anatase–rutile case, setting the X-ray energy below the K absorption edge of titanium (4965 eV) is important in order to avoid unnecessary background from the sample. In such a low-energy case, it is not always easy at normal hard X-ray beamlines at synchrotron radiation facilities to tune X-ray energy to correspond to each lattice parameter. X-ray imaging at the chosen diffraction angle

(i.e., the angle between incident X-rays and normal direction of the camera plane) is much more feasible in such a case.

## CONCLUSIONS

Until now, X-ray diffraction imaging has been attempted by XY scans of the sample, but the biggest problem is the very long measurement time. As discussed in the present article, the use of projection-type imaging is promising. It has become possible to visualize anatase-rich and rutile-rich regions very quickly by simply choosing two different diffraction angles. Mapping of the anatase fraction factor is useful for quantitative discussion. As the present technique can give a 2D image of X-ray diffraction intensity from an inhomogeneous sample, in addition to the anatase–rutile case, many other interesting applications to inhomogeneous complex materials will be considered in the future.

## ACKNOWLEDGMENT

The authors would like to thank Professors Hiroshi Sawa, Yuhsuke Wakabayashi, and Yoshinori Uchida (Photon Factory) for their kind assistance during the experiments. This work was performed with the approval of the Photon Factory Program Advisory Committee (Proposal No. 2002S2-003, 2005G035) and was partly supported by the Active Nano-Characterization and Technology Project, Special Coordination Funds of the MEXT, Japanese Government.

## NOTE ADDED AFTER ASAP PUBLICATION

This paper was published on the Web April 6, 2010 with errors in Figures 1 and 2. The corrected version was reposted April 12, 2010.

Received for review October 24, 2009. Accepted March 23, 2010.

AC9024126

(21) Sakurai, K.; Mizusawa, M. Japanese Patent 3834652, 2006.